Structural and Binding Features of Cofacial Bis-Porphyrins with Calixarene Spacers: Pac-Man Porphyrins That Can Chew

Danica Jokic,[a] Corinne Boudon,[b] Grégory Pognon,[a] Michel Bonin,[c] Kurt J. Schenk,[c] Maurice Gross,*[b] and Jean Weiss*[a]

Abstract: Based on the efficient combination of calixarene spacers and acetylenic porphyrin derivatives, a new generation of cofacial bis-porphyrins has been synthesized. The first crystal structure of a cofacial bis-porphyrin–calixarene conjugate is reported. Their unique architectural features, analogous to those of pac-man-type bis-porphyrins, allow these calixarene–porphyrin conjugates to adapt their shape to the size of bidentate guests, such as diazabicyclo[2.2.2]octane (dabco) and 1,4-pyrazine. The predefined, cofacial arrangement of the porphyrin moieties observed in the solid state and in solution results in extremely high affinities (in the range of $10^9\,M^{-1}$) for these guests. The 1,3-alternate calixarene conformations afford "open-mouth" pac-man structures whose ability to bite on nitrogen bidentates depends on their functionalization. A cone conformer provides a much more flexible structure that exhibits the highest affinity for dabco and pyrazine.

Keywords: calixarenes · host–guest systems · macrocyclic ligands · N ligands · zinc

Introduction

In the early 1980s, cofacial bis-porphyrins were developed with geometrically well-defined spacers, generating the so-called pac-man bis-porphyrins[1] as highly preorganized and geometrically controlled bis-chromophoric systems. These structures are involved in controlled electrochemical processes such as oxygen reduction. Furthermore, for these bis-porphyrins, a precise correlation of structural features with chemical and physical properties has been obtained.[1] Flexible cyclic porphyrin dimers lacking the preorganization of the pac-man porphyrins were developed around the same period. In these species, the cofacial arrangement of the porphyrins was the result of more or less controlled geometric changes, induced by the binding of a bidentate guest (induced fit). The thermodynamics and kinetics associated with these changes have been exhaustively analyzed in the pioneering work of Hunter and Sanders.[2] In the past decade, acyclic forms of porphyrin dimers have received a great deal of attention due to the induction of circular dichroism (CD) when a chiral bidentate is bound to a bis-porphyrinic receptor, which has led to determination of absolute configuration for diamines and amino acids.[3] Flexible structures involving a calixarene platform, in which the cofacial porphyrin arrangement is induced by coordination of bidentate substrates have also been reported recently.[4] Apart from our approach, only two examples in which the calixarene geometry directly affects the porphyrin arrangement have been reported. The first concerns a highly compact tetraporphyrin on a cone calix[4]arene platform.[5] The second involves the use of electrostatic interactions as an assembling tool between cationic porphyrins and anionic calixarenes, and illustrates the potential fine tuning of porphyrin properties by a calixarene spacer.[6]

[a] Dr. D. Jokic, G. Pognon, Dr. J. Weiss
Laboratoire de Chimie des Ligands à Architecture Controlée
Institut de Chimie, Université Louis Pasteur
4 rue Blaise Pascal, 67070 Strasbourg Cedex (France)
Fax: (+33) 390-241-431
E-mail: jweiss@chimie.u-strasbg.fr

[b] Dr. C. Boudon, Prof. M. Gross
Laboratoire d'Electrochimie et de Chimie Physique du Corps Solide
Institut de Chimie, Institut Le Bel, Université Louis Pasteur
4 rue Blaise Pascal, 67070 Strasbourg Cedex (France)
Fax: (+33) 390-24-143
E-mail: gross@chimie.u-strasbg.fr

[c] Dr. M. Bonin, Dr. K. J. Schenk
École Polytechnique Fédérale, LCr1-IMPC-FSB
BPS Dorigny, 1015 Dorigny (Switzerland)

Supporting information for this article is available on the WWW under http://www.chemeurj.org/ or from the author: UV-visible titrations of **2**–**4** with pyrazine and dabco, ^{1}H NMR titrations of receptors **2** and **4** with pyrazine, and ^{1}H NMR titrations of receptor **3** with pyrazine and dabco.

 DOI: 10.1002/chem.200401225

We have developed an efficient synthetic method leading from porphyrin precursor **1** to pac-man-type bis-porphyrin calixarene conjugates **2**–**4** in which a flexible calixarene spacer maintains two porphyrins in a cofacial arrangement.[7] The receptors were designed to cumulate the advantageous preorganization of pac-man bis-porphyrins and the possible fine adjustment of the interchromophore distance of flexible dimers. Indeed, functionalization of the upper rim with two rigidly linked porphyrins affords a cylindrical or cone-shaped calixarene spacer that arranges the two chromophores at a variable distance. The calixarene acts as a hinge that only allows a movement of the two chromophores in the plane containing the acetylenic linkers that connect them to the calixarene platform.

When built on covalently linked calixarene bis-porphyrin tweezers, the pac-man-type bis-porphyrins can bite, and sometimes bite hard. Here we present the structural characterization of such species, together with a study of their biting properties versus typical bidentate axial bases such as diazabicyclo[2.2.2]octane (dabco) and pyrazine (Pyz).

Results and Discussion

Synthesis: The synthetic approach and leading to the species used in this work is described in a preliminary commnication[7] and summarized in Scheme 1. Experimental details of the synthesis of the calixarene precursors and Sonogashira coupling of **1** with functionalized calixarenes are provided in the Experimental Section.

The approach is versatile and allows full control of the 1,3-alternate or cone conformation of the calixarene. The moderate yields (**4**: 35%, **3**: 40%, **2**: 45%) of the double Sonogashira coupling of ethynyl porphyrin derivative **1** with diiodo calixarene precursors **5**, **7**, and **9** are due to steric hindrance around the iodo groups on the calixarene.

X-ray crystallography: Crystals of ligand **4** suitable for X-ray diffraction[8] were obtained by slow diffusion of benzene/hexane into a dilute solution of **4** in dichloromethane. In the structure of the bis-porphyrin (Table 1, Figure 1) the two porphyrin units are in a quasi-cofacial orientation.

This orientation in **4** is opposite to that observed by Smith and Jaquinod[5] in the first upper-rim porphyrin–calixarene conjugate, in which steric crowding generated by the vicinity of four porphyrins forced their respective perpendicular arrangement. Despite the possible free rotation around the ethynyl linker, the two tetrapyrrolic macrocycles are facing each other. The internal crown-6 chain induces opening of the calixarene hinge. Thus, the same dihedral angle of 40° is found between the two phenolic rings of the calixarene that are connected to the porphyrin and between the porphyrin mean planes.

As a consequence, due to the length of the ethynyl linker, the two zinc atoms are 20.522(3) Å apart and are contained roughly in the plane normal to the two tetrapyrrolic macrocycles that contains the two ethynyl linkers. Slight bending of the acetylenic linkages testifies to steric crowding around the edge of the calixarene located between the two porphyrins. Although the zinc atoms are in the plane defined by the four N atoms of each porphyrin ring, oxygen atoms from the neighboring calixcrown-6 units act as a fifth axial ligand. As depicted in Figure 2, the coordination of the oxygen atoms induces a head-to-tail arrangement in the crystal lattice, in which parallel arrays of porphyrins are packed by van der Waals interactions between porphyrin rings belong-

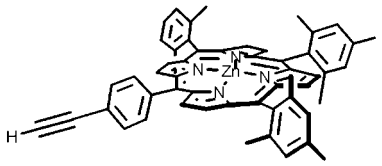

1

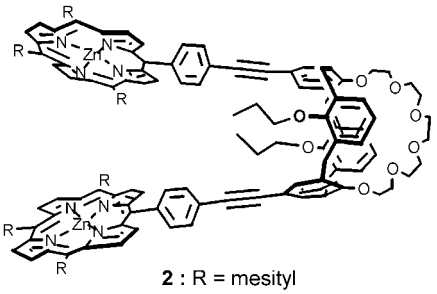

2 : R = mesityl

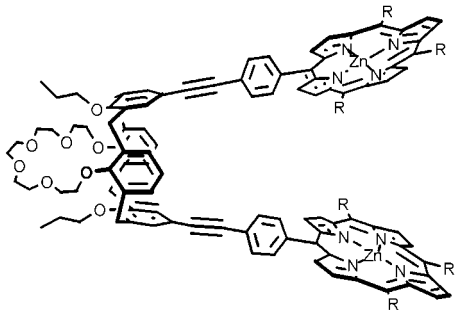

3 : R = mesityl

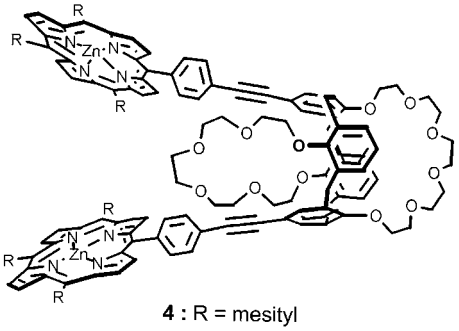

4 : R = mesityl

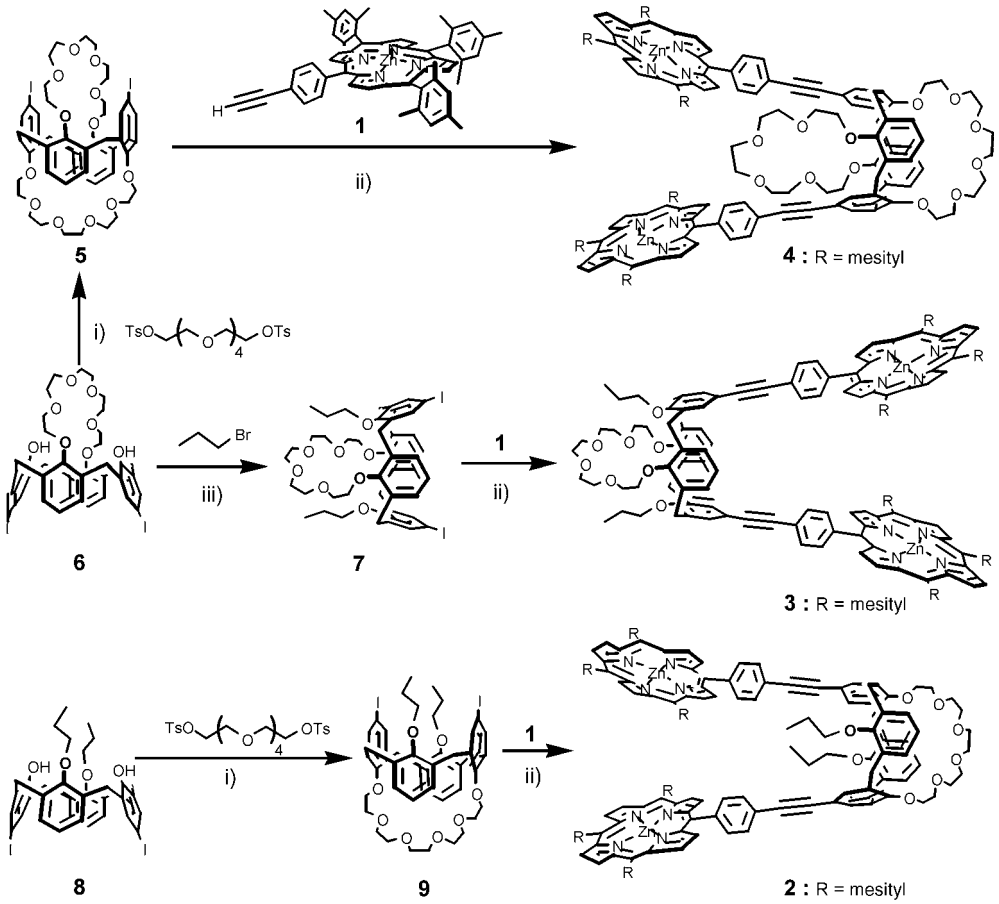

Scheme 1. i) Cs_2CO_3, CH_3CN, reflux: **5** (65%), **9** (60%); ii) 10% $[PdCl_2(PPh_3)_2]$, CuI, NEt_3, 323 K: **4** (35%), **3** (45%), **2** (40%); iii) NaI (cat.), NaH, DMF, 298 K: **7** (75%).

Table 1. Crystallographic data for **1**.[8]

formula	$C_{169.19}H_{148}N_8O_{12}Zn_2$	Z	2
M_r	2615.98	ρ_{calcd} [g cm^{-3}]	1.168
color	red-brown	$\mu(Mo_{K\alpha})$ [mm^{-1}]	0.385
crystal system	triclinic	measured reflns	58904
space group	$P\bar{1}$	unique reflns	27194
a [Å]	17.207(3)	θ range [°]	2.08–26.09
b [Å]	17.717(3)	R_{int}	0.3669
c [Å]	27.198(4)	observed data	4437
α [°]	98.03(2)	R_1,wR_2 [$I>2\sigma(I)$]	0.1157, 0.2035
β [°]	99.113(19)	R_1,wR_2 (all data)	0.4012, 0.2758
γ [°]	111.51(2)	GOF on F^2	0.744
V [Å^3]	7438(2)	parameters	1679

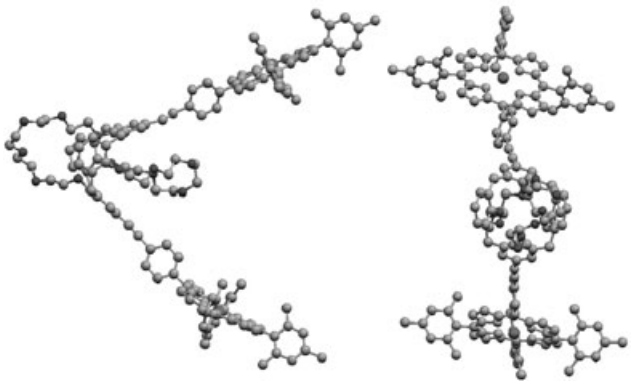

Figure 1. Side and front views of the solid state structure of **4**. Significant distances are discussed in text.

ing to neighboring arrays. It is noteworthy that the solid-state structure correlates quite well with 2D ^{1}H NMR data, which indicate contacts between the central protons of the crown-6 moiety located between the porphyrins and both the β-pyrrolic protons and the protons of the phenyl spacers in the case of **4**.[7] The rather long distance between the two zinc atoms is consistent with the fact that no significant interactions are seen between the two chromophores in the UV-visible spectrum of **4**. When steric crowding between the two chromophores is reduced (in **2** and **3**), interactions occur between the tetrapyrrolic macrocycles. The UV-visible spectra of **1**–**4** show broadening of the Soret band associated with significant hypochromism, especially in the case of **3**, for which the smallest interporphyrin distance is expected.[7]

Determination of association constants: Because of the high degree of preorganization in this series of hosts, a high affin-

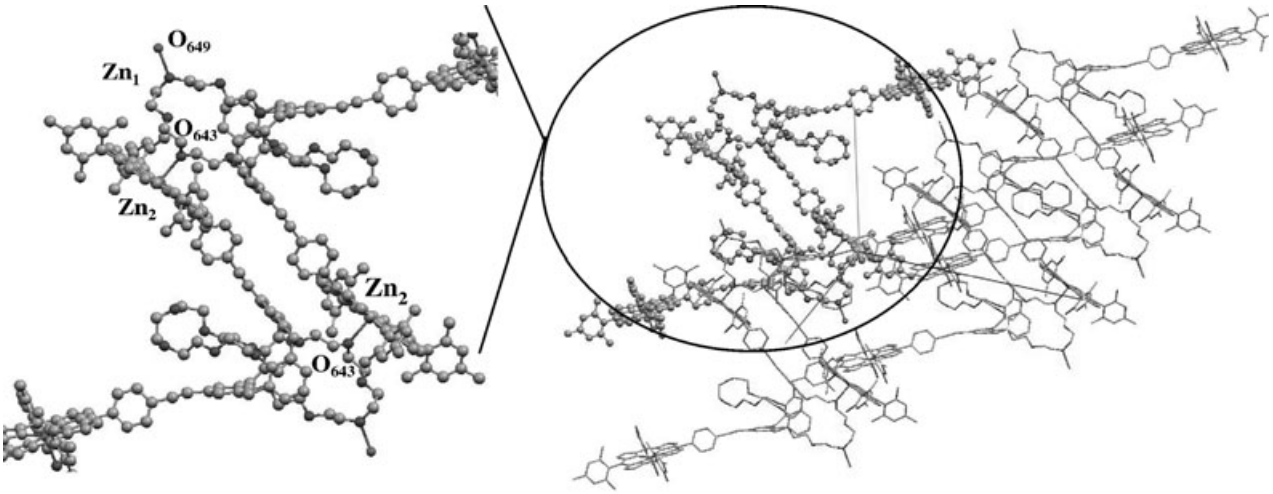

Figure 2. Crystal packing of **4** and zinc(II)–oxygen interactions in the solid state. Solvent molecules (hexane) omitted for clarity.

ity for bidentate axial bases was expected. The ability of **2**–**4** to bind diazabicyclo[2.2.2]octane (dabco) and 1,4-pyrazine was investigated in dichloromethane at 25 °C by UV-visible titrations, ^{1}H NMR spectroscopy, and cyclic voltammetry.

Due to their different geometries, hosts **2**–**4** display very specific binding capabilities. Whereas only one association constant can be calculated for **4** with both dabco and pyrazine, two different host–guest species are observed for both **2** and **3** with each bidentate guest. The association constants determined from UV titrations (see Supporting Information) are collected in Table 2. During the titration process, only a slight red shift of the Soret and Q-bands is observed for each receptor. The binding event corresponds to simultaneous coordination of the substrate to the zinc(II) atom and closing of the tweezers. While the former event is known to produce a large red shift in the range of 10–20 nm, the latter is usually responsible for a blue shift, when occurring in a cofacial arrangement of the porphyrins. For receptors **2**, and **3**, these two effects compensate each other partially, and only small changes in the absorption maxima occur. The differences in the affinities of hosts **2**–**4** for dabco and pyrazine reflects that, in the 1:1 stoichiometry, dabco is a much stronger bidentate ligand due to the presence of two electronically independent nitrogen lone pairs. In contrast, the two nitrogen atoms of the conjugated pyrazine communicate, and the binding of the first nitrogen atom to zinc(II) decreases the basicity of the second. The N–N bond in dabco is shorter (N–N 3.75 Å) than that found in pyrazine (N–N 4.05 Å). As a result of the relative flexibility of the calixarene platform, the strength of the N–Zn coordinative bond governs the affinity of the axial ligand for the bis-porphyrin receptor.

Table 2. Association constants for hosts **2**–**4** with dabco and pyrazine at 298 K in CH_2Cl_2.[a]

	Receptor/dabco		Receptor/pyrazine	
	1:1 [M^{-1}]	1:2 [M^{-2}]	1:1 [M^{-1}]	1:2 [M^{-2}]
2	1.6×10^8	1.0×10^5	0.9×10^6	1.1×10^5
3	7×10^8	1.1×10^4	5.1×10^6	3.7×10^5
4	–	1.2×10^6	–	1.2×10^6

[a] Binding constants obtained from titration of receptor solutions (2.5×10^{-6} M) with substrate solution (2.5×10^{-4} M) from 0 to 50 equiv, analyzed with Specfit[9] (see Supporting Information). No reliable association constant could be determined between **4** and bidentate guests for a 1:1 stoichiometry. 15% errors in association constants.

For each bidentate ligand, the 1:1 host–guest association increases from **2** to **3**. This reflects the greater flexibility and accessibility of the internal cavity of the tweezers in receptors **2** and **3**. The steric constraint imposed by the bis-crown structure of **4** evidently prevents the tweezers from closing around the guest, but consequently promotes the formation of a 1:2 host–guest external monodentate complex for both dabco and pyrazine. For the more flexible species **2** and **3**, the high affinities for dabco and pyrazine also reflect the degree of preorganization of the two zinc porphyrins. The association constants illustrate an impressive enhancement in the stability of 1:1 inclusion complexes in comparison to previously reported association constants between dabco and pyrazine with other flexible bis-porphyrins. Early results from Sanders and Hunter showed that cyclophane-type porphyrin dimers bind pyrazine and dabco with associations constants on the order of 10^2 and $10^6\,M^{-1}$, respectively.[2a] In this case, an induced-fit process was observed in which the linear character of the bidentate guest was responsible for the final cofacial arrangement of the chromophores. Recently, more highly preorganized porphyrin–calixarene conjugates have been designed in which an increase by one order of magnitude in the association constants with dabco ($1.0\times10^7\,M^{-1}$) is observed.[4b] The smallness of this increase in association constant reflects that, in these hosts, the porphyrins are attached to the calixarene platform lower rim through flexible amide bonds and O-alkylation. Indeed, the energy cost for adequate orientation of the porphyrins in the host precludes strong enhancement of association. As shown by the association constants listed in Table 2, hosts **2** and **3**

clearly have a high degree of preorganization that leads to a gain three orders of magnitude greater than in flexible porphyrin dimers. As a result of the rigid connection of the porphyrins to the calixarene hinge, complexation of dabco and pyrazine occurs without energy-wasting geometric changes in the receptors. This interpretation is confirmed by data from ^{1}H NMR spectroscopic monitoring of dabco and pyrazine binding in receptors **2**–**4**.

Binding geometry in bis-porphyrin tweezers: ^{1}H NMR titrations at 298 K in $CDCl_3$ have been performed for receptors **2**–**4** with both guests. In both cases, similar conclusions can be drawn from the analysis of chemical shift displacements. Only the results of dabco binding with hosts **3** and **4** are commented on in detail.

Figure 3 shows the evolution of the ^{1}H NMR spectrum of **3** on addition of dabco. All signals are well defined throughout the titration, and this provides evidence for a slow exchange process between bound and free receptor when the ratio r=[dabco]/[**3**] is between 0 and 1. For r=0.33 and 0.66, the dabco singlet appears at −4.5 ppm and denotes the insertion of the bidentate base in between the porphyrin rings of the tweezers. All dabco present is bound to the receptor. The signals corresponding to free host disappear concomitantly, and at r=1 no free species are observed in solution. Most signals assigned to the porphyrin β-pyrrolic protons are shielded, which is consistent with shortening of the distance between the tetrapyrrolic macrocycles on guest complexation. Protons H_a and H_b are respectively shifted to 8.3 and 8.45 ppm. $H_{a'}$ and $H_{b'}$ are also shielded and appear in the set of signals around 7.2 ppm. This indicates a more severe pinching of the bis-porphyrin in the neighborhood of the calixarene upper rim than on the open end of the tweezers.

Protons of the phenyl spacer are also shifted, with H_c now appearing at δ=7.4 ppm, and H_d being less shielded ($\Delta\delta$=−0.35 ppm) at δ=7.8 ppm. The dabco signal appears at δ=−4.5 ppm until 1:1 stoichiometry is reached. At r>1, the dabco peak rapidly broadens then disappears completely, while the rest of the spectrum remains unchanged. Even on addition of a large excess of substrate (r=10), no additional changes are observed in the host's spectrum. This is consistent with a persistent closed form of the tweezers, in which the excess substrate induces fast exchange of the bound dabco with free species. Considering the differences between the association constant of the 1:1 and 1:2 complexes of **3** with dabco, it is not surprising that external coordination of dabco, leading to a 1:2 complex, is not observed by NMR spectroscopy at r=10, because larger excesses are required to destroy the 1:1 complex. A similar behavior is observed for receptor **2**, for which the signal due to dabco bound within the tweezers disappears in the presence of

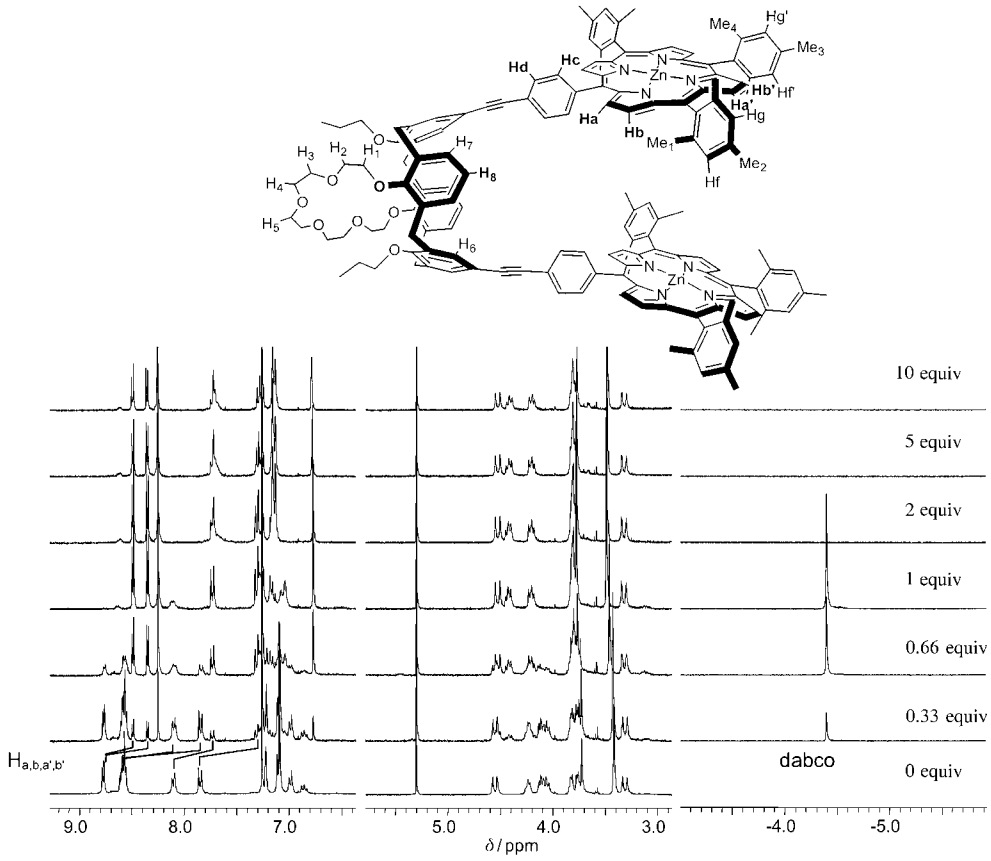

Figure 3. NMR titration of **3** with dabco ($CDCl_3$, 300 MHz, 298 K).

excess substrate, whereas the signals due to the receptor protons remain unaffected. In both cases, total disruption of the 1:1 complexes requires a very large excess of dabco. The signal due to free dabco significantly perturbs the resolution of the ^{1}H NMR spectra. In contrast, in receptor **4**, rapid disruption of the 1:1 complex is observed in the presence of excess substrate.

In the case of weakly bound substrates, the spectral behavior of the host is drastically different, as shown by the spectral evolution in Figure 4 for titration of **4** with dabco. The addition of dabco to a solution of **4** induces broadening of the signals, which is clear evidence for exchange between free and bound **4** that is slow on the NMR timescale. However, some displacements of the signals are noticeable and may be assigned to conformational changes similar to those observed with host **3**, but less pronounced due to weaker association. An extremely broad signal centered at -4.5 ppm can be detected up to $r=1$, but disappears rapidly on addition of even a slight excess of substrate. After the changes that occur for $0<r<2$, protons of the receptor are observed close to their original chemical shifts. The slight differences observed are assigned to a persistent complex in a 2:1 form. Due to an association constant of approximately $10^6\,\text{M}^{-1}$, it is anticipated that an excess of five dabco per binding site (10 equiv) is needed to observe the fully complexed form, as depicted in Figure 4.

The ^{1}H NMR results can be analyzed in light of the association constants determined by UV-visible titrations. Depending on the calixarene conformation and its functionalization, the flexibility of the calixarene hinge can be assessed, and the selectivity of the binding can be explained. For hosts **2**–**4**, binding properties are summarized in Scheme 2, in which the symbolism RS_{in} stands for complexation of substrate S in the tweezers R, and RS_{out} stands for complexation of the substrate outside the tweezers.

For host **4**, it is clear that steric hindrance due to the internal crown-6 ether chain disfavors pinching of the tweezers to accommodate coordination of the bidentate substrate for $r\leq 1$. Therefore, on guest addition, weak insertion is observed only for dabco. No association constant could be determined for the 1:1 complex due to competition with the favored formation of the 1:2 complex. However, ^{1}H NMR titration shows the presence of a broad signal centered at -4.5 ppm that is indicative of dabco binding within the bisporphyrin tweezers, with fast exchange between bound and unbound species. As soon as r exceeds 1, this signal disappears and the host's signals sharpen and appear at their original chemical shifts. Thus, as suggested by ^{1}H NMR spectroscopy, an intermediate insertion complex with dabco may be postulated, but cannot be further characterized in the case of host **4**.

Hosts **2** and **3** can accommodate both bidentate guests due to greater flexibility of the calixarene platform. The

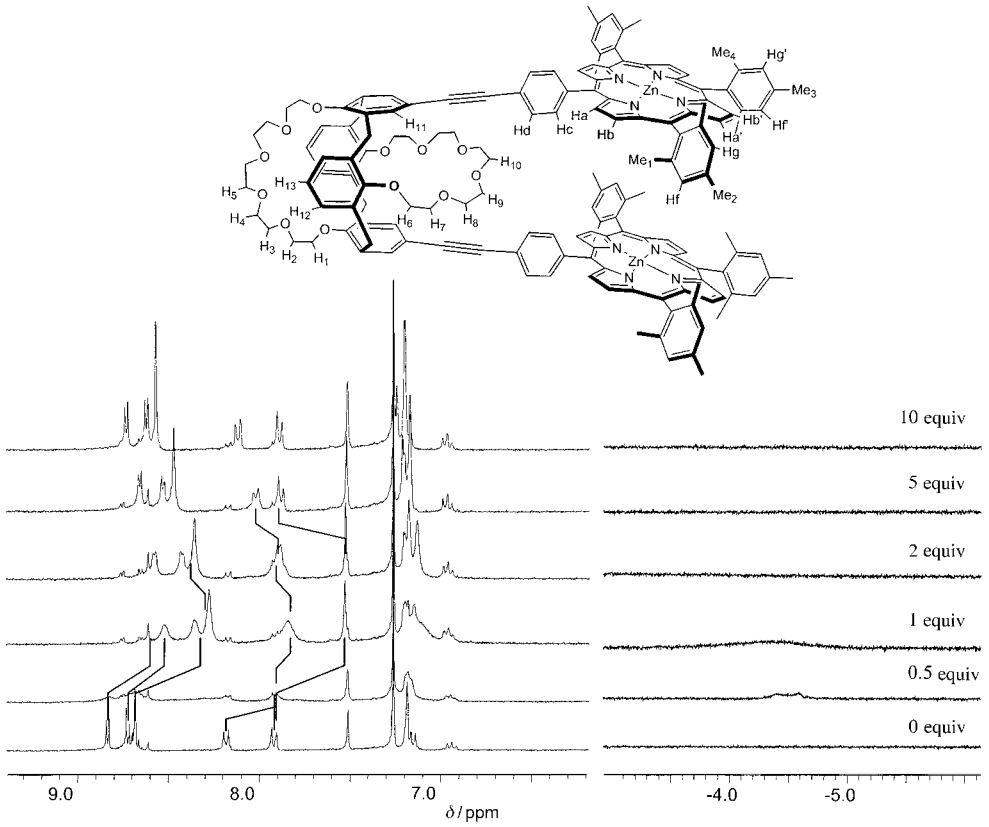

Figure 4. NMR titration of **4** with dabco ($CDCl_3$, 300 MHz).

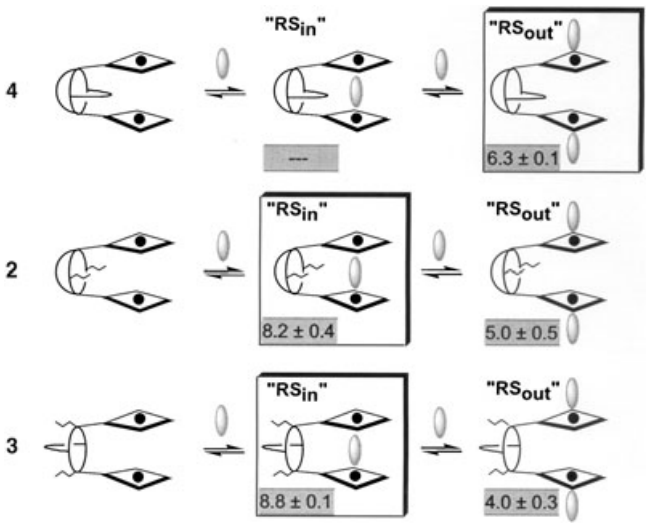

Scheme 2. Dabco binding modes and lg K_{assoc} for hosts **2**–**4**.

large association constants determined from UV-visible titrations for the 1:1 complexes, and their comparison with the association constants corresponding to the 1:2 forms, imply that at NMR concentrations and with up to a tenfold excess of guests, only species corresponding to the favored 1:1 complexes are observed. For these more flexible hosts, the signals corresponding to the crown ether chain and to the CH_2 bridges of the calixarene structure are also affected by addition of the bidentate ligand, indicative of changes in the geometry of the platform.

Electrochemical studies: Electrochemical studies confirm the binding scheme depicted for dabco in Scheme 2. The behavior of pyrazine complexes was not studied by electrochemistry because pyrazine is inactive over the range of potentials for which these studies were carried out.[10] Uncoordinated dabco exhibits only one irreversible oxidation step at 0.36 V versus ferricinium/ferrocene (Fc^+/Fc).

To eliminate any contribution of ohmic drop to the peak current variations, all peak currents reported here were obtained by convolution voltammetry. For each receptor, the current intensity I_{pC} of the first two-electron reduction at E_C can be used as a reference for the current intensities I_p of the free and bound receptor oxidations and the sum of the I_p values associated with $E_{Ox1(RS)}$ and $E_{Ox1'(RS)}$.

For all receptors, independent of their respective affinities for dabco, Scheme 3 explains the possible evolutions during the oxidation and back-reduction processes. Not all of these steps are observed for each receptor. The peculiar electrochemical behavior of each receptor pinpoints that the influence of dabco binding in an oxidized receptor is significantly different than in the receptor itself.

Figure 5a shows the convolution voltammograms of all receptors in the absence of dabco. Figure 5b–f show their respective responses in the presence of increasing amounts of dabco. In all cases, the addition of dabco immediately induces the rise of a new, reversible oxidation signal $E_{Ox(RS)}$, between 0.250 and 0.300 V. This is assigned to the first oxidation of (ZnP-S-ZnP), which is facilitated by coordination of dabco to zinc. The behavior of receptors **2**–**4** can be analyzed in light of the respective affinities of **2**–**4** for dabco, keeping in mind that the zinc porphyrin radical cations ($ZnP^{\bullet+}$) have higher affinities for dabco than the neutral species. In the absence of dabco, the receptors display a classical set of two reversible oxidations. The first oxidation occurs at $E_{OxR} = 0.310$ V for **2** and at 0.360 V for **3** and **4**. The second oxidation is at 0.700 V for all receptors. The change in the shape of the first oxidation peaks is consistent with the weak excitonic coupling observed in UV absorption, which showed that, while the ZnP chromophores are independent in **4**, they interact in **2** and even more so in **3**. This increasing interaction results in a split-induced broadening of the first oxidation peak for **2** and **3**. Due to the small separation of these potentials (< 59 mV), interactions between the porphyrins can only be detected by the measurement of truncated I_p values for **2** and **3**.

As expected, the behavior of receptors **2** and **3** is similar when $-1 < n < 0$ (Scheme 3), for which the RS_{in} coordination mode is exclusive, as no S_{out} oxidation at 0.560 V could be observed (Figure 5b). Indeed, based on the oxidation potentials of the receptors, RS_{in} and RS_{out} coordination modes cannot be distinguished. In contrast, oxidations characteristic of the substrate are only observed if the substrate is bound outside (RS_{out}). Insertion within the tweezers prevents oxidation of both nitrogen atoms in the substrate.

In substoichiometric amounts, the presence of dabco inside the tweezers facilitates only one zinc porphyrin oxidation compared to that in the free receptor at $E_{Ox1} = 0.190$ V, and $E_{Ox1} = 0.240$ V for **3** and **2**, respectively. The second zinc porphyrin oxidation remains at an unchanged potential of $E_{Ox1'(RS)} = E_{OxR} = 0.360$ V in the case of **3**, and $E_{Ox1'(RS)} = E_{OxR} = 0.310$ V in the case of **2**. This lack of influence on the second zinc porphyrin can be ascribed either to a poor electron-donating character of the substrate in the $(RS_{in})^{\bullet+}$ form, or to decoordination of dabco from the remaining neutral zinc porphyrin to generate the ($ZnP^{\bullet+}$-S)-(ZnP) species depicted in Scheme 3. A split back-reduction is observed at $E_{Red1(RS)} = 0.190$ V and $E_{Red1'(RS)} = E_{RedR} = 0.360$ V for **3**, and at $E_{Red1} = 0.010$ V and $E_{Red1'(RS)} = E_{RedR} = 0.240$ V for **2**, in which E_{RedR} corresponds to free ($ZnP^{\bullet+}$), and

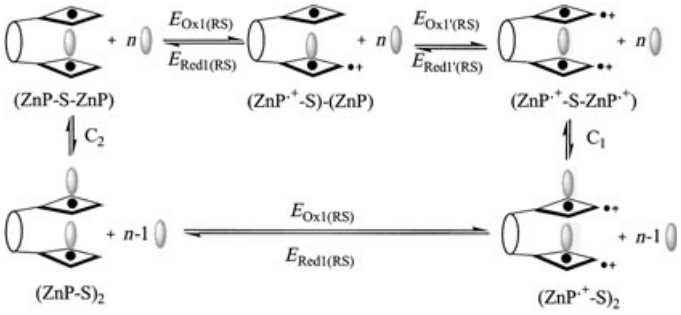

Scheme 3. Redox and thermodynamic equilibria observed by cyclic voltammetry.

$E_{Red1(RS)}$ to reduction of the monodentate ($ZnP^{\bullet+}$-S) complex in the RS_{in} or RS_{out} conformation. Due to its higher affinity for dabco, receptor **3** shows only a small shift of its back-reduction at $E_{Red1(RS)} = 0.190$ V, which reflects that even in the ($ZnP^{\bullet+}$-S-$ZnP^{\bullet+}$) state, dabco is bound to both Zn porphyrins. Receptor **2** shows its weaker affinity for dabco in the rise of a clearly more difficult back-reduction that corresponds to the monodentate $Zn(P^{\bullet+})$-dabco complex at $E_{Red1(RS)} = 0.010$ V. As expected, dabco binding to receptor **4** has little influence on the oxidation potentials. In reduction, the peak corresponding to reduction of the monodentate ($ZnP^{\bullet+}$-S) complex is clearly seen at $E_{Red1(RS)} = 0.010$ V, which is the same potential as in the case of **2**. In the presence of one equivalent of dabco (Figure 5c), receptor **3** displays a unique broad oxidation peak at 0.220 V that corresponds to a combination of the $E_{Ox1(RS)} = 0.190$ V cathodically shifted oxidation induced by formation of a bidentate dabco complex for the first porphyrin in (ZnP-S-ZnP). At $E_{Ox1'(RS)} = 0.360$ V, oxidation of the second porphyrin in the ($ZnP^{\bullet+}$-S)-(ZnP) species in which dabco is still weakly bound to the neutral ZnP moiety is observed. Receptor **2** shows a similar displacement, but with a marked shoulder at 0.140 V due to pronounced monodentate behavior of dabco. The oxidation of the second zinc porphyrin moiety in the tweezers remains at $E_{Ox1'(RS)} = 0.290$ V, close to its original value of 0.310 V. In addition to the unaffected zinc porphyrin oxidation at $E_{Ox1'(RS)} = 0.370$ V, receptor **4** shows two facilitated oxidations, a shoulder at 0.190 V for the monodentate RS_{out} form and a peak at $E_{Ox1(RS)} = 0.300$ V for the monodentate RS_{in} form. From the affinity constants of receptor **4** for dabco, and the observation of a large NMR peak at high field for its 1:1 complex, the presence of RS_{in} and RS_{out} at this stoichiometry explains the observation of the two facilitated oxidations. However, these oxidations cannot be unambiguously assigned to a precise conformer. Nonetheless, it is logical to assume that the cathodically shifted oxidation is due to a pure monodentate RS_{out} form of dabco rather than a weak, bidentate RS_{in} conformer. This hypothesis is strongly supported by the presence of a return peak observed for the oxidation of the RS_{out} form, but not for the RS_{in} conformer, which is destabilized by oxidation of the first ZnP moiety. In all forms, a monoelectronic, cathodically shifted return peak is observed for the monodentate dabco form ($ZnP^{\bullet+}$-S)-(ZnP), together with a monoelectronic reduction of the free ($Zn^{\bullet+}$P) moiety released from the ($ZnP^{\bullet+}$-S-$ZnP^{\bullet+}$) species.

Figure 5d confirms these trends for all receptors in the presence of two equivalents of dabco, and provides some additional evidence for the specific behaviors of **2**, **3**, and **4**. In particular, the disappearance of all reduction peaks corresponding to the free ($Zn^{\bullet+}$P) moiety is consistent with the interpretation of all of the observed processes described above. Indeed, on oxidation of the first (ZnP-S) moiety at $E_{Ox1(RS)}$ in the (ZnP-S-ZnP) species, the second (ZnP) moiety is oxidized in a substrate-free state at $E_{Ox1'(RS)}$ to generate an electron-poor ($Zn^{\bullet+}$P) that quickly binds the second dabco molecule. For receptors **2** and **3**, a small oxidation peak of bound dabco is observed, that is, some dabco binding in the ($ZnP^{\bullet+}$-S-$ZnP^{\bullet+}$) species takes place outside of the tweezers. This is even more pronounced for receptor **4**, even though dabco oxidation is partially masked by the shifted, dielectronic second oxidation of the $(ZnP^{\bullet+}\text{-S})_2$ species, which is easily identified by its reversibility. The change that corresponds to the enhanced affinity of $\mathbf{4}^2(^{\bullet+})$ for two dabco molecules appears at much lower dabco/receptor ratios for **4** than for **2** or **3**. Thus, the affinities of the $(ZnP^{\bullet+})_2$ species for dabco can be considered to follow the same trend as the affinities in the neutral receptors **2**–**4**. Figure 5e and d confirm the evolution, and show that for receptor **3** in the RS_{in} conformation, the dabco-binding behavior, which involves switching from bidentate/monodentate/bidentate in the respective 1/1 complexes (ZnP-S-ZnP), ($ZnP^{\bullet+}$-S)-(ZnP), and ($ZnP^{\bullet+}$-S-$ZnP^{\bullet+}$), is not perturbed, even in the presence of five equivalents of dabco.

Thus, the electrochemical response of receptor **3** in the presence of one equivalent of dabco is a stepwise process in which the RS_{in} status of the complex is maintained throughout the redox cycle. The first zinc porphyrin oxidation generates a bis-porphyrin species in which the two porphyrins are now distinct. Oxidation of the second zinc porphyrin generates a bis(radical cation) that displays a strong affinity for dabco in the RS_{in} mode. In addition to this electrochemically induced chewing motion, it is remarkable that two identical chromophores can be differentiated efficiently by the addition of one equivalent of a bridging substrate, due to the particular flexibility of the calixarene bridge that connects them. These aspects are particularly interesting for the design of systems capable of storing information, because the presence of dabco preferentially bound to the radical cation may prevent intra- and intermolecular diffusion of the charge located on the oxidized species in films incorporating these species.

Conclusion

The flexibility and the versatile coordinating properties of the bis-porphyrin hosts presented here demonstrate that the fine-tuning of physicochemical properties can be achieved through small geometrical changes by using flexible calixarene platforms for positioning and orienting porphyrins. The orientation postulated in solution is observed in the solid state, and 2D NMR measurements provide evidence for similarities between solid-state and solution structures. High affinities for bidentate substrates have been observed in the most flexible structures, and NMR changes in the calixarene region on complexation of these guests suggest that geometrical changes affecting the chromophore arrangement occur through geometrical changes of the tetraphenolic hinge. The use of the complexing abilities of the calixarene moiety for modulating interporphyrin interactions is currently being explored.

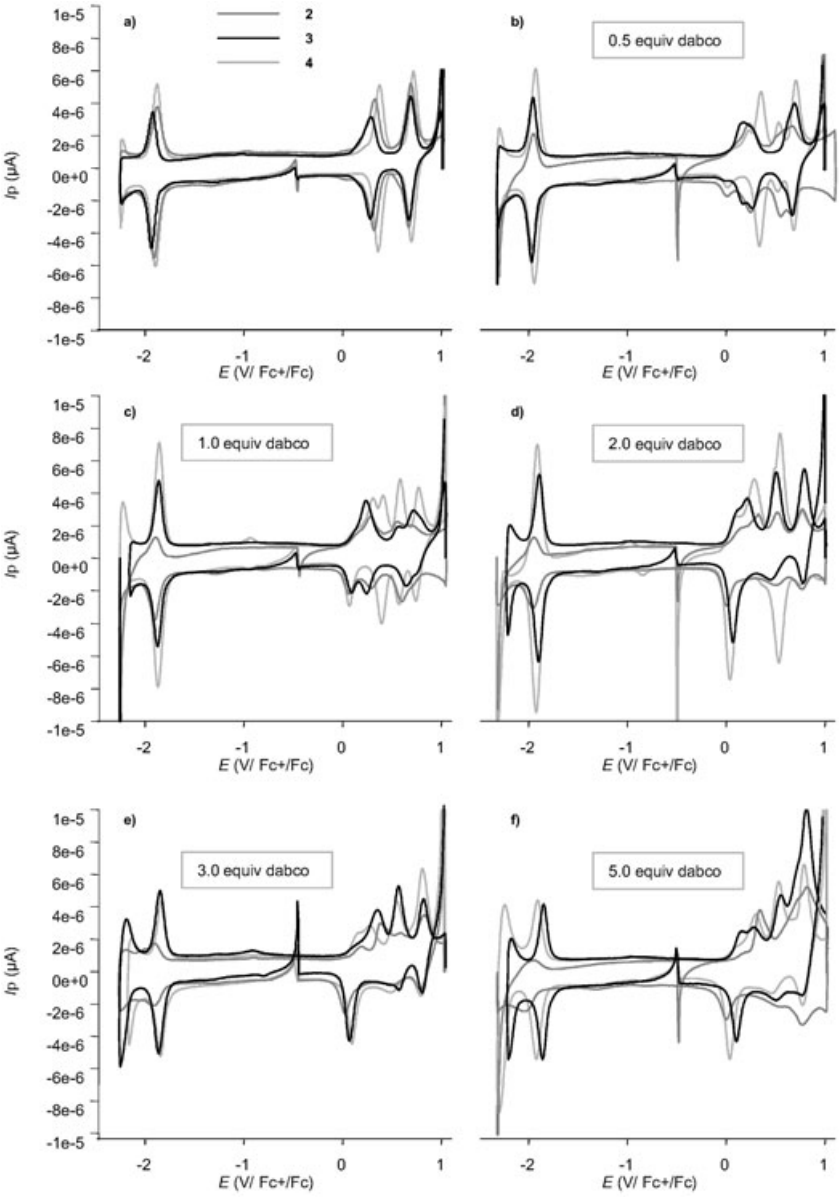

Figure 5. Evolution of convolution voltammetry curves for receptors **2**–**4** in the presence of increasing amounts of dabco.

Experimental Section

All solvents were dried prior to use. Acetonitrile was distilled under an argon atmosphere from CaH_2 and stored over 4 Å molecular sieves. Dimethylformamide (DMF) was pre-dried by azeotropic distillation with toluene prior to standing over 4 Å molecular sieves. Toluene was dried by standing over sodium chips. All reagents were commercial except calixarenes **6** and **8**, which were iodinated according to literature procedures.[11] ^{1}H NMR spectra were recorded on Bruker Avance 300 and Avance 500 spectrometers and the chemical shifts were calibrated on residual nondeuterated solvent ($\delta = 7.27$ ppm for $CHCl_3$ in $CDCl_3$). UV-visible spectra were obtained on a Hewlett Packard diode-array (HP 8453) spectrophotometer in 1 cm cells.

Synthesis of compound 5: An excess of Cs_2CO_3 (0.115 g, 0.336 mmol) and pentaethylene glycol di-*p*-toluenesulfonate (0.110 g, 0.202 mmol) were added to a solution of **6** (0.1 g, 0.112 mmol) in CH_3CN (30 mL) under argon. The reaction mixture was refluxed for 24 h. Then, CH_3CN was removed under reduced pressure, and the residue extracted with CH_2Cl_2 and 10% aqueous HCl. The organic phase was separated and washed with water. After evaporation of the solvent, the product was purified by column chromatography (Al_2O_3, CH_2Cl_2/AcOEt, 80/20) (0.8 g, 0.072 mmol, 65%). M.p. >250°C; ^{1}H NMR (300 MHz, $CDCl_3$, 25°C): $\delta =$ 7.41 (s, 4H; ArH), 7.08 (d, $J = 7.5$ Hz, 4H; ArH), 6.88 (t, $J = 7.5$ Hz, 2H; ArH), 3.8 (s, 8H; $ArCH_2Ar$), 3.73 (m, 9H; $ArOCH_2CH_2OCH_2CH_2$), 3.59 (m, 14H; $ArOCH_2CH_2OCH_2CH_2$), 3.42 (t, $J =$ 12.9 Hz, 4H; $ArOCH_2CH_2OCH_2CH_2$), 3.36 (t, $J = 12.9$ Hz, 4H; $ArOCH_2CH_2OCH_2CH_2$), 3.03 ppm (t, $J = 12.9$ Hz, 4H; $ArOCH_2CH_2OCH_2CH_2$); elemental analysis (%) calcd for $C_{48}H_{58}I_2O_{12}$: C 53.34, H 5.41; found: C 53.60, H 5.44.

Synthesis of compound 7: NaH (0.005 g, 0.24 mmol), *n*-bromopropane (0.196 g, 1.16 mmol), and NaI (0.023 g, 0.16 mmol) were added to a solution of **6** (0.07 g, 0.08 mmol) in DMF (30 mL) under argon. The reaction mixture was stirred at room temperature for 8 h. Then aqueous 10% HCl (50 mL) was slowly added, and the resulting solid was filtered and washed with water. Pure product was obtained by recrystallization from MeOH (0.04 g, 0.042 mmol, 50%). M.p. >250°C; ^{1}H NMR (300 MHz, $CDCl_3$): $\delta = 7.11$ (d, $J = 7.3$ Hz, 4H; ArH), 7.00 (t, $J =$ 7.3 Hz , 2H; ArH), 6.53 (s, 4H; ArH), 4.34 (d, $J = 13.5$ Hz, 4H; $ArCH_2Ar$), 4.04 (t, $J = 7.5$ Hz, 4H; $OCH_2CH_2CH_3$), 3.71–3.3.68 (m, $ArOCH_2CH_2OCH_2CH_2$), 3.15 (d, $J = 13.5$ Hz, 4H; $ArCH_2Ar$), 1.93 (m, 4H; $OCH_2CH_2CH_3$), 1.08 ppm (t, $J = 7.3$ Hz, 6H; $OCH_2CH_2CH_3$); elemental analysis (%) calcd for $C_{44}H_{52}I_2O_8 \cdot 2\,MeOH \cdot H_2O$: C 52.88, H 5.98; found: C 52.53, H 5.63.

Synthesis of compound 9: An excess of Cs_2CO_3 (0.63 g, 1.95 mmol) and pentaethylene glycol di-*p*-toluenesulfonate (0.65 g, 1.16 mmol) were added to a solution of **8** (0.5 g, 0.65 mmol) in CH_3CN (50 mL) under argon. The reaction mixture was refluxed for 24 h. Then CH_3CN was removed under reduced pressure, and the residue extracted with CH_2Cl_2 and aqueous 10% HCl. The organic phase was separated and washed with water, and the solvent was evaporated. Crystallization of the oily residue from CH_2Cl_2/MeOH yielded **9** as a white solid (0.4 g, 1.14 mmol, 65%): M.p. >250°C; ^{1}H NMR (300 MHz, $CDCl_3$, 25°C): $\delta = 7.36$ (s, 4H; ArH), 6.84 (d, $J = 7.5$ Hz, 4H; ArH), 6.82 (t, $J = 7.5$ Hz, 2H; ArH), 3.8 (s, 8H; $ArCH_2Ar$), 3.73–3.44 (m, $ArOCH_2CH_2OCH_2CH_2$), 1.46 (t, 6H; $OCH_2CH_2CH_3$), 0.93 ppm (m, 4H; $OCH_2CH_2CH_3$); elemental analysis (%) calcd for $C_{44}H_{52}I_2O_8 \cdot 2\,CH_2Cl_2 \cdot$ MeOH: C 48.47, H 5.19; found: C 48.34, H 4.84.

Synthesis of receptor 2: Porphyrin **1** (0.132 g, 0.160 mmol) and calix[4]arene **9** (0.07 g, 0.073 mmol) were placed in a flask which was thoroughly flushed with argon. Degassed toluene and NEt_3 (10 mL) were then added, as well as catalytic amounts of $[PdCl_2(PPh_3)_2]$ and CuI (10 mol%). The reaction mixture was stirred at 50°C for 16 h. The sol-

vents were removed under reduced pressure. The organic layer was washed with water and dried over Na_2SO_4. The product was purified by column chromatography (SiO_2, CH_2Cl_2/acetone 80/20). Yield: 0.068 g, 0.03 mmol, 40%; m.p. >250°C; ^{1}H NMR (500 MHz, CD_2Cl_2, 25°C): δ = 8.84 (d, J = 4.5 Hz, 4H; $H_{\beta pyr}$), 8.70–8.65 (m, 12H; $H_{\beta pyr}$), 8.17 (br d, J = 7.6 Hz, 4H; ArH), 7.90 (d, J = 7.6 Hz, 4H; ArH), 7.45 (s, 4H; ArH_{calix}), 7.26 (s, 4H; ArH_{xylyl}), 7.15 (s, 8H; ArH_{xylyl}), 7.14 (d, J = 7.8 Hz, ArH_{calix}), 6.90 (t, J = 7.8 Hz, ArH_{calix}), 3.94 (t, J = 15.8 Hz, 4H; $ArOCH_2CH_2OCH_2$-CH_2OCH_2), 3.91 (t, J = 15.8 Hz, 4H; $ArOCH_2CH_2OCH_2CH_2OCH_2$), 3.65 (br s, 8H; $ArCH_2Ar$), 3.57 (m, 4H; $ArOCH_2CH_2O$), 3.53 (s, 4H; $ArOCH_2CH_2OCH_2CH_2OCH_2$), 3.45 (t, J = 14.5 Hz, 4H; $OCH_{2Propyl}$), 3.29 (m, 4H; $ArOCH_2CH_2O$),2.59–2.58 (2 s, 12H; $ArCH_3$), 2.47 (s, 12H; $ArCH_3$), 1.71 (s, 6H; $ArCH_3$), 1.56 (s, 24H; $ArCH_3$), 1.19 (m, 4H; $OCH_2CH_{2propyl}$), 0.83 ppm (m, 6H; $OCH_2CH_2CH_3$); FAB positive MS: m/z calcd for $C_{154}H_{142}O_8N_8Zn_2$: 2362.5; found: 2362.9 [M^+]; elemental analysis (%) calcd for $C_{154}H_{142}O_8N_8Zn_2{\cdot}3CH_2Cl_2{\cdot}C_6H_{14}$: C 72.21, H 6.52, N 3.91; found: C 72.39, H 6.04, N 4.14; UV/Vis (CH_2Cl_2) λ_{max} (ε) = 422 (700000), 551 nm (36000 $mol^{-1}dm^3cm^{-1}$).

Synthesis of receptor 3: Porphyrin **1** (0.120 g, 0.132 mmol) and calix[4]arene **7** (0.06 g, 0.06 mmol) were placed in a flask which was thoroughly flushed with argon. Degassed toluene and NEt_3 (5 mL) were then added, as well as catalytic amounts of [$PdCl_2(PPh_3)_2$] and CuI (10 mol%). The reaction mixture was stirred at 50°C for 3 h. The solvents were removed under reduced pressure. The organic layer was washed with water and dried over Na_2SO_4. The product was purified by column chromatography (SiO_2, CH_2Cl_2/acetone, 95/5). Yield: 0.05 g, 0.021 mmol, 35%); m.p. >250°C; ^{1}H NMR (500 MHz, CD_2Cl_2, 25°C): δ = 8.77 (d, J = 4.6 Hz, 4H; $H_{\beta pyr}$), 8.57 (d, 4.6 Hz, 4H; $H_{\beta pyr}$), 8.49 (d, J = 4.6 Hz, 4H; $H_{\beta pyr}$), 8.46 (d, J = 4.6 Hz, 4H; $H_{\beta pyr}$), 8.08 (d, J = 8 Hz, 4H; ArH), 7.82 (d, J = 4 Hz; ArHH), 7.22 (s, 4H; ArH_{xylyl}), 7.18 (d, J = 8 Hz, 4H; ArH_{calix}), 7.02 (s, 8H; ArH_{xylyl}), 6.98 (t, J = 8 H; 2H; ArH_{calix}), 6.97 (s, 4H; ArH_{calix}), 4.58 (d, J = 13.6 Hz, 4H; $ArCH_2Ar$), 4.28 (t, J = 7.5 Hz, 4H; $ArOCH_2CH_2O$), 4.17 (t, J = 7.5 Hz, 4H; $ArOCH_2CH_2O$), 3.96 (t, J = 8 Hz, 4H; $ArOCH_2CH_2CH_3$), 3.79 (m, 4H; $ArOCH_2CH_2OCH_2CH_2OCH_2$), 3.71 (m, 4H; $ArOCH_2CH_2OCH_2CH_2OCH_2$), 3.68 (s, 4H; $ArOCH_2CH_2OCH_2$-CH_2OCH_2), 3.34 (d, J = 13.6 Hz, 4H; $ArCH_2Ar$), 2.58 (s, 6H; $ArCH_3$), 2.42 (s, 12H; $ArCH_3$), 2.03 (q, J = 8 Hz, $ArOCH_2CH_2CH_3$), 1.71 (s, 12H; $ArCH_3$), 1.52 (s, 24H; $ArCH_3$), 1.09 ppm (t, J = 8 Hz, $ArOCH_2CH_2CH_3$); FAB positive MS: m/z calcd for $C_{154}H_{142}O_8N_8Zn_2$: 2362.5; found: 2363.6 [M^+]; elemental analysis (%) calcd for $C_{154}H_{142}O_8N_8$-$Zn_2{\cdot}2CH_2Cl_2{\cdot}CH_3COCH_3$: C 73.69, H 5.91, N 4.32; found: C 74.01, H 5.92, N 3.93; UV/Vis (CH_2Cl_2) λ_{max} (ε) = 420 (665000), 550 nm (29000 $mol^{-1}dm^3cm^{-1}$).

Synthesis of receptor 4: Porphyrin **1** (0.1 g, 0.117 mmol) and calix[4]arene **5** (0.06 g, 0.053 mmol) were placed in a flask that was thoroughly flushed with argon. Then degassed toluene and NEt_3 (10 mL) were added, as well as catalytic amounts of [$PdCl_2(PPh_3)_2$] and CuI (10% mol.). The reaction mixture was stirred at 50°C for 16 h. The solvents were removed under reduced pressure. The organic layer was washed with water and dried over Na_2SO_4. The product was purified by column chromatography (SiO_2, CH_2Cl_2/acetone 90/10). Yield: 0.04 g, 0.16 mmol, 30%; m.p. >250°C; ^{1}H NMR (500 MHz, CD_2Cl_2): δ = 8.88 (d, J = 4.7 Hz, 4H; $H_{\beta pyr}$), 8.76 (d, J = 4.7 Hz, 4H; $H_{\beta pyr}$), 8.69–8.64 (m, 8H; $H_{\beta pyr}$), 8.2 (m, 4H; ArH), 7.93 (m, 4H; ArH), 7.48 (s, 4H; ArH_{calix}), 7.46 (s, 4H; ArH_{xylyl}), 7.30 (s, 4H ArH_{xylyl}), 7.28 (s, 2H; ArH_{xylyl}), 7.10 (s, 2H; ArH_{xylyl}), 7.28 (t, J = 7.5 Hz, ArH_{calix}), 6.90 (t, J = 7.5 Hz, ArH_{calix}),4.05–3.02 (m, 32H; $ArOCH_2CH_2OCH_2CH_2OCH_2$), 3.72 (br s, 8H; $ArCH_2Ar$), 3.62 (s, 4H; $ArOCH_2CH_2OCH_2CH2OCH_2$), 3.57 (s, 4H; $ArOCH_2CH_2OCH_2CH_2OCH_2$), 2.62 (s, 12H; $ArCH_3$),2.61 (s, 6H; $ArCH_3$), 2.48 (s, 6H; $ArCH_3$), 1.86 (s, 6H; $ArCH_3$), 1.82 (s, 18H; $ArCH_3$), 1.76 ppm (s, 6H; $ArCH_3$); FAB MS: m/z calcd for $C_{158}H_{148}O_{12}N_8Zn_2$: 2481.6; found: 2479.8 [M^+]; elemental analysis (%) calcd for $C_{158}H_{148}O_{12}N_8Zn_2{\cdot}4CH_2Cl_2{\cdot}2H_2O$: C 68.69, H 5.64, N 3.92; found: C 68.24, H 6.06, N 3.86; UV/Vis (CH_2Cl_2) λ_{max} (ε) = 422 (940000), 551 nm (44000 $mol^{-1}dm^3cm^{-1}$).

Acknowledgement

We are indebted to the CNRS for financial support. D.J. thanks the French Ministry of Foreign Affairs (MAE) for a Ph.D. fellowship.

[1] For the early work, see C. K. Chang, I. Abdalmuhdi, *J. Org. Chem.* **1983**, *48*, 5388–5390; for a review, see J. P. Collman, P. S. Wagenknecht, J. E. Hutchinson, *Angew. Chem.* **1994**, *106*, 1620–1639; *Angew. Chem. Int. Ed. Engl.* **1994**, *33*, 1537–1556; and for a recent example, see Y. Deng, C. J. Chang, D. J. Nocera, *J. Am. Chem. Soc.* **2000**, *122*, 410–411.

[2] a) H. L. Anderson, C. A. Hunter, M. N. Meah, J. K. M. Sanders, *J. Am. Chem. Soc.* **1990**, *112*, 5780–5789; b) C. A. Hunter, M. N. Meah, J. K. M. Sanders, *J. Am. Chem. Soc.* **1990**, *112*, 5773–5780.

[3] a) G. Proni, G. Pescitelli, X. Huang, K. Nakanishi, N. Berova, *J. Am. Chem. Soc.* **2003**, *125*, 12914–12927; b) V. V. Borovkov, G. A. Hembury, Y. Inoue, *Angew. Chem.* **2003**, *115*, 5468–5472; *Angew. Chem. Int. Ed.* **2003**, *42*, 5310–5314, ; c) G. Proni, G. Pescitelli, X. Huang, N. Q. Quraishi, K. Nakanishi, N. Berova, *Chem. Commun.* **2002**, 1590–1591; d) V. V. Borovkov, J. M. Lintuoluoto, Y. Inoue, *Org. Lett.* **2002**, *4*, 169–171; e) X. Huang, K. Nakanishi, N. Berova, *Chirality* **2000**, *12*, 237–255; f) Q. Yang, C. Olmsted, B. Borhan, *Org. Lett.* **2002**, *4*, 3423–3426.

[4] a) M. Dudic, P. Lhotak, I. Stibor, K. Lang, P. Proskova, *Org. Lett.* **2003**, *5*, 149–152; b) M. Dudic, P. Lhotak, H. Petrickova, I. Stibor, K. Lang, J. Sykora, *Tetrahedron* **2003**, *59*, 2409–2415; c) L. Baldini, P. Ballester, A. Casnati, R. M. Gomila, C. A. Hunter, F. Sansone, R. Ungaro, *J. Am. Chem. Soc.* **2003**, *125*, 14181–14189; d) S. Shinkai, M. Ikeda, A. Sugasaki, M. Takeuchi, *Acc. Chem. Res.* **2001**, *34*, 494–503.

[5] R. G. Khoury, L. Jaquinod, K. Aoyagi, M. M. Olmstead, A. J. Fisher, K. M. Smith, *Angew. Chem.* **1997**, *109*, 2604–2607; *Angew. Chem. Int. Ed. Engl.* **1997**, *36*, 2497–2500, .

[6] a) L. Di Costanzo, S. Geremia, L. Randaccio, R. Purrello, R. Lauceri, D. Sciotto, F. G. Gulino, V. Pavone, *Angew. Chem.* **2001**, *113*, 4375–4377; *Angew. Chem. Int. Ed.* **2001**, *40*, 4245–4247; b) G. Moschetti, R. Lauceri, F. G. Gulino, D. Sciotto, R. Purrello, *J. Am. Chem. Soc.* **2002**, *124*, 14536–14537.

[7] D. Jokic, Z. Asfari, J. Weiss, *Org. Lett.* **2002**, *4*, 2129–2132.

[8] A dark red-brown crystal of dimensions 30×30×150 μm was measured on a Stoe IPDS system with Mo radiation at 130 K. A crystal to image plate distance of 70 mm was chosen, and two hundred images, in oscillation steps of 1°, were exposed for sixty minutes each. An inspection of reciprocal space ascertained that the diffraction figure consisted essentially of the spots corresponding to the cell given in Table 1, but some powdery components were present as well, and the data were very weak. For the integration, a mosaic spread of 0.015 and a constant spot size of 13 pixels were used. The intensities were corrected for Lorentzian and polarization effects, but no absorption correction was deemed necessary. The decay during the measurement was negligible. The structure was solved and refined with the help of SHELXTL 5.05.[12] All non-hydrogen atoms except the solvent molecules were refined anisotropically, and all hydrogen atoms, which were made to ride on their associated carbon atoms, and the solvent molecules isotropically. Owing to the low parameter/observation ratio 502 restraints had to be imposed on the molecule. CCDC 225260 contains the supplementary crystallographic data for this paper. These data can be obtained free of charge from The Cambridge Crystallographic Data Centre via www.ccdc.cam.ac.uk/data_request/cif.

[9] R. A. Binsteadt, A. D. Zuberbülher, Specfit, A Program for Global Least Squares Fitting of Equilibrium and Kinetics Systems Using Factor Analysis & Marquardt Minimisation, Version 2-11 C, 1998, Spectrum Software Associates, Chapel Hill.

[10] All measurements were performed in CH_2Cl_2 + 0.1 M tetrabutylammonium hexafluorophosphate ($TBAPF_6$) with a glassy carbon electrode (∅ 3 mm) connected to a PGSTAT20 Autolab potensiostat (ECO chemie BV-NL Utrecht), a Pt counterelectrode, and an Ag/

AgCl reference electrode. Typical host (receptor R) concentrations of 10^{-4} M were used in a 5 mL cell. Potentials were calibrated after final addition of ferrocene to the solution before the last CV scan.

[11] B. Klenke, W. Friedrichsen, *J. Chem. Soc. Perkin Trans. 1* **1998**, 3377–3380.

[12] G. M. Sheldrick, SHELXTL 5.05, Bruker Analytical X-Ray Instruments, Inc. Madison, WI (**1996**).

Received: November 30, 2004
Published online: April 29, 2005

